Proceedings of the 16th International IEEE Annual Conference on Intelligent Transportation Systems (ITSC 2013), The Hague, The Netherlands, October 6-9, 2013

Selective Salient Feature based Lane Analysis

R. K. Satzoda and Mohan M. Trivedi

***Abstract*— Lane analysis involves data-intensive processing of input video frames to extract lanes that form a small percentage of the entire input image data. In this paper, we propose lane analysis using selective regions (LASeR), that takes advantage of the saliency of the lane features to estimate and track lanes in a road scene captured by on-board camera. The proposed technique processes selected bands in the image instead of the entire region of interest to extract sufficient lane features for efficient lane estimation. A detailed performance evaluation of the proposed approach is presented, which shows that such selective processing is sufficient to perform lane analysis with a high degree of accuracy.**

I. Introduction

Lane estimation and tracking is considered to be one of the most vital component of all intelligent driver safety systems (IDSS) owing to the role lanes play in understanding the environment outside the vehicle [1]. There are a number of vision-based lane analysis methods reported in literature as shown in recent works like [2], [3], [4], [5], [6], [7], [8], [9] etc., which usually involve lane feature extraction, outlier removal and tracking using Kalman/particle filters. A variety of techniques like using steerable filters [2], learning based approaches [6], color information [5] etc. are used to extract lane features by processing the input image frames. The lane features thus obtained are further analyzed using outlier removal techniques and tracking to improve the accuracy and robustness of the lane analysis process. Fig. 1 shows the typical lane analysis approach. It is noteworthy that lane features form less than 5% of the entire image but most existing lane analysis techniques process the entire image frame to extract the lane features. This not only increases computation time but also leads to an overkill of computing resources, and both these metrics are critical metrics for realizing efficient on-board lane analysis systems.

In this paper, we ask the question: Why do we need to process the entire image frame to extract less than 5% of the valuable information? We derive inspiration from from studies in selective saliency directed processing of human vision [10], [11] to propose a selective salient feature based lane analysis method. The proposed approach does not process the entire image looking for lane features. Instead, we devise a selective approach that looks for salient lane features in limited but necessary number of places in the image, and capturing salient features that give a good indication that they are indeed lane features. We also show how the conventional road and vehicle models and lane tracking techniques can still function with acceptable accuracy but with selected salient lane features, instead of all possible lane features that are used in existing methods.

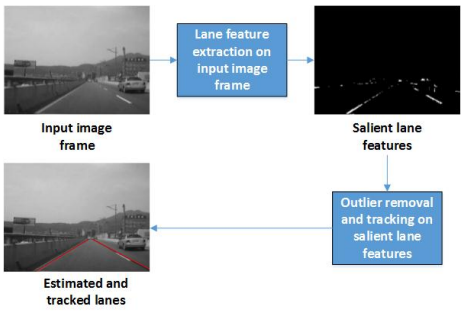

Fig. 1. Typical lane analysis approach involves analyzing the entire input image frame to extract salient lane features in the image that are further processed to estimate and track lanes in the road scene

The rest of the paper is organized as follows. We take a look at some related and recent lane analysis methods in Section II. The proposed selective lane analysis approach is presented in Section III. A detailed evaluation of the proposed method in terms of its accuracy and performance, and its tradeoffs is presented in Section IV followed by conclusions drawn in Section V.

II. Related Work

A detailed survey of various lane analysis techniques is presented in [2] and more recently in [8]. One of more complete lane analysis techniques in recent times is VioLET that was proposed in [2] uses steerable filters for detecting directional lanes. Road and vehicle models with Kalman filtering to robustly estimate and track lanes. One of the main contributions in this work is a quantitative method to evaluate the lane analysis performance. Another recent work that uses steerable filters is the integrated lane and vehicle detection approach by Sayanan et al in [9]. In this approach lanes and vehicles are used to detect each other more deterministically because of the driving property that vehicles are usually localized within their lanes.

While [2], [9] take advantage of the gradient information of the lanes on the road surface, [5] uses the color property of the lanes to extract lanes from roads. Different color spaces are used to differentiate lanes from road surface in [5]. Another approach to detecting lanes is proposed in [6], which employs Haar-like and Gabor filter-based feature extractors to detect lane features. A cascaded classifier is further used to confirm the presence of lane features.

Another approach to lane analysis is presented in [3] recently which uses does a two-level lane feature extraction

R. K. Satzoda and Mohan M. Trivedi are with University of California San Diego, La Jolla, CA, USA. rsatzoda@eng.ucsd.edu, mtrivedi@ucsd.edu

978-1-4799-2914-613/$31.00 ©2013 IEEE

step followed by outlier removal using RANSAC. The two-level lane feature extraction involves an adaptive thresholding that highlights the lane features, which are collected using a coarse-grained Hough transform. The candidates are further analyzed at specific points along the lines indicated by Hough transform using a correlation operation using a Gaussian-like template.

These are some of the complete and robust lane analysis techniques. A more detailed listed of techniques, their advantages and disadvantages is presented in [8]. A study of these existing method showed that all these methods process the entire image (or a region of interest defined by the lower half of the image) to select a few lane feature points, which are processed further. Though [3] scans for lane features at specific points in the image, the pre-processing stage involves full image scan and computations like Hough transform. In most of these methods, the saliency of the lane features is not fully exploited to extract them from the image in a selective manner.

III. Proposed Lane Analysis Approach - LASeR

In this section, we describe LASeR - lane analysis using selective regions. As discussed earlier, it is proposed to process the input video frames in a selective manner, keeping in view the saliency of lane features. LASeR will first extract sufficient lane features from selected regions in the image, that will then be used for lane estimation and tracking.

A. Selective Band-based Lane Feature Extraction

In this method, instead of processing the entire image or an RoI (usually the lower part of the image) for extracting lane features as shown in [2], we propose to use N_s number of scan bands that are only w_B pixels in height. It will be shown that processing sufficient number of such scan bands and extracting lane features in these bands gives acceptable levels of lane detection accuracy.

The first step in LASeR is to transform the input image into the inverse perspective mapping domain (IPM) [12]. We apply steerable filters in selected scan bands in the IPM image to extract lane features efficiently.

1) Steerable Filters on Scan-bands in IPM Image: In [13], steerable filter for any arbitrary orientation is derived in the following way. Given a Gaussian filter $G(x,y)$ as:

$$G(x,y) = e^{-\frac{x^2+y^2}{\sigma^2}}, \tag{1}$$

we have the derivatives of $G(x,y)$ along x and y direction given by

$$G_x(x,y) = \frac{\partial}{\partial x}G(x,y) = \frac{-2x}{\sigma^2}e^{-\frac{x^2+y^2}{\sigma^2}} \tag{2}$$

$$G_y(x,y) = \frac{\partial}{\partial y}G(x,y) = \frac{-2y}{\sigma^2}e^{-\frac{x^2+y^2}{\sigma^2}} \tag{3}$$

The filter response for any angle can be computed using $G_x(x,y)$ and $G_y(x,y)$ using the following equation:

$$G^{\theta}(x,y) = G_x(x,y)\cos\theta + G_y(x,y)\sin\theta \tag{4}$$

In [2], the angles for which the steerable filters give maximum/minimum response, is determined by maximizing/minimizing the above equation to give θ_{min} and θ_{max} at every pixel coordinate in the image domain, which are given by:

$$\theta_{max} = arctan(\frac{G_{xx}-G_{yy}-A}{2G_{xy}}) \tag{5}$$

$$\theta_{min} = arctan(\frac{G_{xx}-G_{yy}+A}{2G_{xy}}) \tag{6}$$

where $A = \sqrt{G_{xx}^2 - 2G_{xx}G_{yy} + G_{yy}^2 + 4G_{xy}}$. These maxima angles are used to find the image pixel coordinates that are along the lane markings and extract possible lane features. This involves computation of θ_{max} for every pixel in the image domain in order to capture the varying lane orientation in the image domain.

The following steps are employed in the proposed lane feature extraction step of LASeR such that the image is processed selectively and yet extract sufficient lane features information for further processing.

1) The image I is converted to IPM image I_W.
2) N_s scan bands are selected from I_W, each of height w_B (called as scan-band height henceforth).
3) In each scan band B_i, we look for response to *vertical* steerable filters only.
4) The steerable filter response obtained from the previous step in each band is then subjected to what we call a shift-and-match operation, that extracts lane features from steerable filter response.
5) These selected features from each scan band are then sent to outlier removal using road models and lane tracking.

We will now elaborate on the above steps. Firstly, unlike in the image domain, IPM domain gives a more regular lane formation. This advantage has been used in various lane estimation methods but for the purpose of outlier removal after finding initial lane features. In the proposed method, we take advantage of the regular and predictable nature of the lanes in IPM domain from the very beginning. We select N_s scan bands from the IPM image I_W. Considering that each scan band height is only w_B pixels, the lanes will appear as short vertical segments with each scan band. This is shown in Fig. 2. This vertical appearance is also because the angular variations of the lanes is predictably towards 0^o (vertical direction) in the IPM image. Therefore, applying vertical steerable filters on the scan bands will amplify the lane edges. There will be other non-lane features also that could also be selected but they will be eliminated in the next step. Therefore, instead of find the maximum angle at every image pixel coordinate, we propose to apply on $G^{0^\circ}(x,y)$ filter to a selected set of pixels in each band of the IPM image. From (4) & (1), we get,

$$G^{0^\circ}(x,y) = G_x(x,y) = \frac{-2x}{\sigma^2}e^{-\frac{x^2+y^2}{\sigma^2}} \tag{7}$$

Convolving $G^{0^\circ}(x,y)$ with pixels in each scan band B_i, we

have the steerable filter response B_i^S, i.e.,

$$B_i^S = B_i \otimes G^{0^\circ}(x,y). \tag{8}$$

The filter response B_i^S of each scan band is now examined for lane features using the proposed shift-and-match operation.

2) Shift-and-Match Operation (SMO) for Lane Feature Extraction: The filter response B_i^S in each band captures gradient changes along the vertical direction. In order to eliminate filter responses due to non-lane edges, we first apply two thresholds T_+ and T_- on B_i^S. These thresholds capture two different kinds of intensity transitions in B_i^S. T_+ captures dark to light transition, whereas the T_- captures light to dark transition. The result binary maps are denoted as E_+ and E_-. Fig. 2 shows the result of the two thresholds on the steerable filter response of upper scan band selected in the IPM image in Fig. 2.

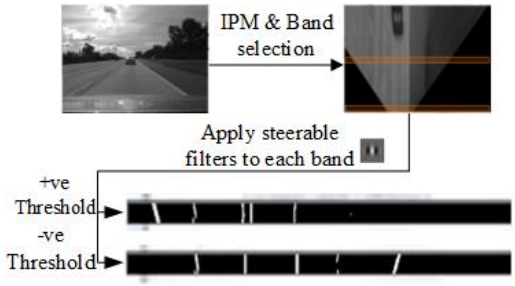

Fig. 2. Generating steerable filter output from bands.

It can be seen that E_+ and E_- have non-lane features also. We now propose *shift-and-match* operation (SMO) to extract lane features and eliminate non-lane features from each band. In order to do this, we compute the horizontal projection vectors $\mathbf{p}_+$ and $\mathbf{p}_-$ for E_+ and E_-, i.e. for scan band of w_B pixels high and N_B pixels wide, we have

$$\mathbf{p}_+ = \left[\sum_{k=1}^{w_B} E_+(1,k), \sum_{k=1}^{w_B} E_+(2,k), \ldots \sum_{k=1}^{w_B} E_+(N_B,k)\right] \tag{9}$$

$$\mathbf{p}_- = \left[\sum_{k=1}^{w_B} E_-(1,k), \sum_{k=1}^{w_B} E_-(2,k), \ldots \sum_{k=1}^{w_B} E_-(N_B,k)\right] \tag{10}$$

Peaks are formed in these projection vectors where there are clusters of pixels in E_+ and E_-. Fig. 3 shows the plot of $\mathbf{p}_+$ and $\mathbf{p}_-$ for the band that was thresholded in Fig. 2.

Lane marking feature has the following property: *it has two intensity transitions, dark→light followed by light→dark and separated by a fixed number of pixels δ in the IPM image I_W*. Therefore, the peaks corresponding to the lane edges in $\mathbf{p}_+$ and $\mathbf{p}_-$ are also separated by a small δ. In order to capture these pairs of transitions of lanes, $\mathbf{p}_+$ is shifted by δ places to the left and multiplied with $\mathbf{p}_-$ resulting in the vector $\mathbf{K}_{B_i}$ for scan band B_i, i.e.,

$$\mathbf{K} = (\mathbf{p}_+ << \delta) \odot \mathbf{p}_- \tag{11}$$

where $\odot$ represents point-wise multiplication. We call this the shift-and-match operation (SMO). Fig. 3 shows the result of the shift and match operation performed on $\mathbf{p}_+$ and $\mathbf{p}_-$ for the upper band selected in Fig. 2. It can be seen that

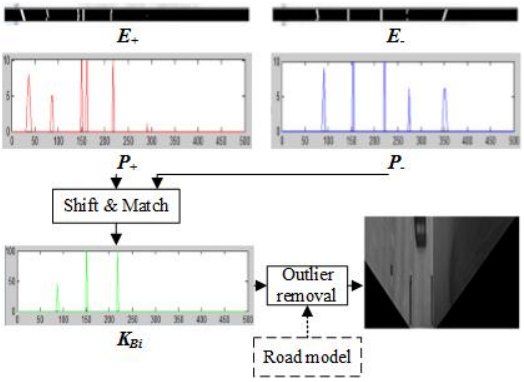

Fig. 3. Illustrating shift and match operation for band B_i

SMO eliminates most of the peaks that are formed by non-lane features and retains the peaks corresponding to the lane features in B_i. In Fig. 3, the peak locations correspond to the dark to light transition edge of the lane feature markings in Fig. 2 for both the left and right lanes of the host lane. The locations of the peaks in $\mathbf{K}_{B_i}$ for each scan band B_i are then used along with the road model and lane tracker to eliminate non-lane outliers that may be picked up by SMO (because of them having similar properties as the lane features).

B. Outlier Removal & Lane Tracking

The band-based lane feature extraction step gives positions of possible lane markings in each band. Let P_{B_i} denote the set of coordinates of possible lane markings in each band B_i, i.e.,

$$P_{B_i} = [P_{1i}(x_1,y_i), P_{2i}(x_2,y_i), \ldots, P_{ki}(x_k,y_i), \ldots, P_{N_i,i}(x_{N_i},y_i)] \tag{12}$$

where $P_{ki}(x_k,y_i)$ denotes the k-th coordinate of a lane feature in the i-th scan band, and N_i is the total number of lane marking features detected in the i-th scan band. Therefore, we get N_s such arrays corresponding to the N_s scan bands. This is illustrated for $N_s = 3$ in Fig. 4. These lane features points in each scan band must now be associated with each other across scan bands to visualize the correct lanes and eliminate any non-lane outliers that may been picked up by SMO in the previous step. In order to do this, we apply the clothoid road model illustrated in [2] to associate the positions of the lane features across bands. Referring to the road model shown in Fig. 4, the clothoid model gives the x-coordinate in the IPM given the vehicle deviation ϕ from the center of the lane and the y-coordinate (vertical axis) using the following equation:

$$X_W = \phi + \theta Y_W + C Y_W^2 \tag{13}$$

where (X_W, Y_W) is a world coordinate of a point in the IPM image, ϕ is the lateral deviation of the vehicle from the center of the lane, C is the curvature of the road and θ is the yaw angle of the vehicle. The last two parameters, i.e. C and θ are obtained from the vehicle dynamics captured using CAN bus. When (X_W, Y_W) are calibrated with the IPM image scale, we

978-1-4799-2914-613/$31.00 ©2013 IEEE

get the corresponding (x_w, y_w) coordinates in the IPM image domain.

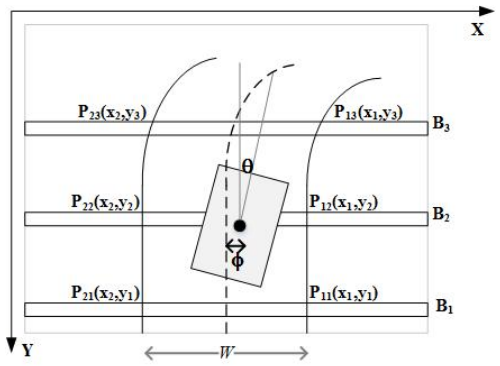

Fig. 4. Vehicle and clothoid road model as seen in world coordinate system (or IPM image domain) is shown. The y-coordinates of the scan bands in the proposed method are used to estimate the possible location of the lane feature points in each scan band using the clothoid road model defined by (13).

In LASeR, we apply this road model to remove outliers (non-lane features) that are picked in each scan band. Unlike existing techniques, which apply the road model to all the feature points that possibly form the lane in the image, we apply the road model to the points that are found in each scan band, i.e. the points in each P_{B_i}. This reduces the computational cost tremendously as compared to conventional way of applying the road model to eliminate outliers and visualize the lanes. Therefore, in LASeR, (13) is applied to the lane feature coordinates collected in P_{B_i}. This is illustrated in Fig. 4, wherein the y-coordinates of the scan bands are used to estimate the possible location of the lane feature points in each scan band using the clothoid road model that is defined by (13). Any lane feature point in P_{B_i} that does not satisfy the road model is eliminated. The same model can be extended further to detect neighboring lanes also, but this is out of scope of this paper.

The above method of outlier removal using the road model is effective, if we can determine the lateral deviation of the vehicle ϕ in the lane accurately. In order to do this, the proposed method uses the lane feature positions of the scan band that is closest to the ego-vehicle, i.e. scan band B_1 in Fig. 4. However, depending on the presence of lane markings and type of lane markings, the lowermost scan band B_1 may not always detect the lane features. In order to continuously track the lane features in scan band B_1 (so that we can track the features in the other scan bands also), we apply Kalman filter tracking to the lane features obtained in the lower most scan band. It was observed that the lowermost scan band is the most predictable in terms of the lane features as compared to the upper bands and hence tracking the lane markings is effective in getting the lane positions continuously across time. These lane positions can then be used to determine the lateral offset of the vehicle in the lane, i.e. ϕ. The Kalman filter used for tracking the center of the vehicle in the lane is defined by the following state variables:

$$x_{k+1|k} = Ax_{k|k} \quad \text{and} \quad y_k = Mx_k \tag{14}$$

where x, A and M are defined as follows:

$$x = [\phi, \tan\theta, W]^T \tag{15}$$

$$A = \begin{bmatrix} 1 & v\Delta t & 0 \\ 0 & 1 & 0 \\ 0 & 0 & 1 \end{bmatrix} \quad ; \quad M = \begin{bmatrix} 1 & 0 & 0 \\ 0 & 1 & 0 \\ 0 & 0 & 1 \end{bmatrix} \tag{16}$$

In the above equations, ϕ is the lateral deviation of the car from center of the lane, θ is the yaw angle of the car, v is the vehicle speed and W is the width of the lane. The yaw angle and vehicle speed are obtained from the CAN bus. The world coordinates of the left and right lanes X_W^l and X_W^r are approximated using the following equations [9]:

$$X_W^l = \phi - \frac{1}{2}W \quad ; \quad X_W^r = \phi + \frac{1}{2}W. \tag{17}$$

X_W^l and X_W^r are then calibrated to the IPM image domain to the lanes in the IPM image. Inversing the IPM results in visualizing the lanes in the image domain.

IV. Performance Evaluation

In this section, LASeR is evaluated using the test video datasets obtained by LISA-Q2 testbed [14], that is equipped with a front facing camera that captures 640×480 video sequences at nearly 20 frames per second. The vehicle dynamics that are used for lane tracking and road model fitting are captured using the in-vehicle CAN-bus. Test video sequences were captured under different lighting and road conditions, freeways and urban roads. Table I lists the different datasets (each with a minimum of 250 frames) that are used for evaluation. In addition to these datasets, we also captured 6000 frame video sequence on the freeway for the evaluating lane localization, which will be discussed next.

TABLE I
Dataset Description

Set 1	Freeway lanes		Set 2	Freeway with vehicles	
Set 3	Freeway concrete surface		Set 4	Freeway circular reflectors	
Set 5	Urban road with shadows				

A. Evaluation of Lane Localization

LASeR was evaluated for lane localization using the evaluation method described in [2]. In order to do this, we fixed a downward facing camera equipped with a wide angle lens on the left side of the testbed. This camera captures the left lane marking with minimal perspective distortions. More details about ground truth generation can be found in

978-1-4799-2914-613/$31.00 ©2013 IEEE

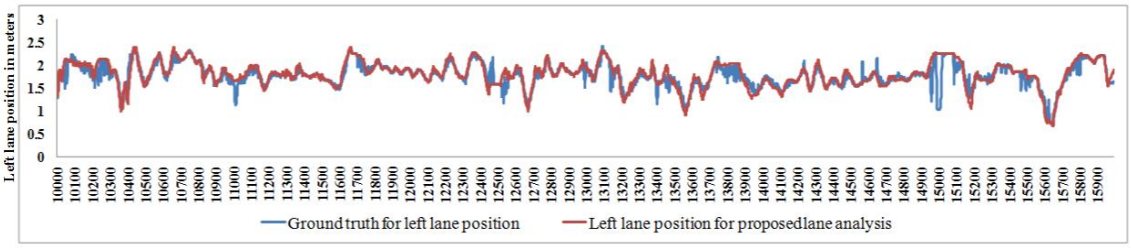

Fig. 5. Evaluation of ego-vehicle localization of the proposed lane tracking technique against ground truth data.

[14]. The test run for evaluation was conducted on a freeway in California state and a sequence comprising 6000 frames was used for evaluating the lane markings that are extracted by the proposed lane analysis technique. We consider the positions of left lane feature from the scan band that is closest to the ego vehicle for evaluation against the ground truth data.

Fig. 5 shows the lane localization of the left lane with respect to the front facing camera (i.e. the middle of the car). It can be seen that for most part of the drive, the left lane marking detected by LASeR using the selected scan bands follows the ground truth position for the left lane. The average absolute error between the two is found be less than 8 centimeters. There are some instances where we see large deviations from the ground truth. All those deviations were found to be when the vehicle were drifting to the next lane or changing lanes.

B. Evaluation of Detection Rates

Firstly, Fig. 6 shows some sample images with lanes that are extracted from complex road scenes by applying LASeR on input images from the datasets listed in Table I. It can be seen that LASeR is able to extract lanes in varying lane conditions like cracks (Fig. 6(a)-(c)), presence of vehicles (Fig. 6(d)), presence of strong shadows (Fig. 6(e)-(g)). The proposed method is also able to extract lanes with circular reflectors as shown in Fig. 6(e)&(f), and on Korean roads as shown in Fig. 6(h).

Fig. 7 shows detection accuracy results in datasets 1, 2 and 3, in which we are evaluating the detection of dashed lane markings (i.e. no circular reflectors or solid lane boundaries). The effect of changing the number of scan bands and the scan band height on detection accuracy is shown in Fig. 7. It is evident that reducing the number of scan bands will reduce the detection accuracy of the lane features because depending on the position of the lane marker and the speed of the vehicle, the scan band at a particular coordinate may fail to detect the lane marking (which we consider as failed detection). Therefore, having more number of scan bands increases the detection rate as seen in Fig. 7 for both cases of the scan band height, i.e. 10 and 5 pixels. The detection accuracy with 8 scan bands is over 90% in all test datasets. This is an important observation because this implies that for the IPM images of size 360×500, processing just 8 scan lines with 10 pixels each is sufficient to get a detection rate of 95%, instead of processing the entire 360×500 sized image

Fig. 6. Sample results of lane detection by LASeR in complex road scenes: (a) curved road with linear edges and lane like markings, (b)&(c) uneven road surface with linear features along the lane markings, (d) presence of overtaking vehicles, (e) circular reflectors and shadows, (f) circular reflectors and faint lanes under heavy shadow, (g) lanes on urban roads with frequent shadows, (h) Korean lanes.

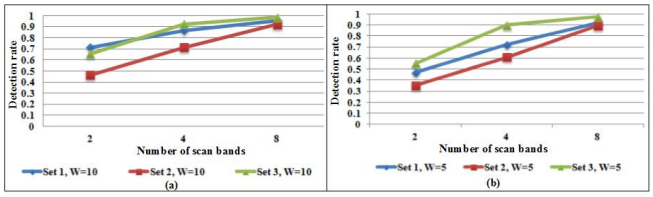

Fig. 7. Detection rate versus number of scan bands for scan band height = 10 in (a) and 5 in (b).

(which is usually the case in most conventional methods). This figure also plots the detection accuracy for varying scan band height, i.e. $w_B = 10$ and 5 in Fig. 7(a) & (b) respectively. A higher scan band captures more information, implying better detection rate. Therefore, it is expected that bands with height of 5 pixels have lesser detection rate. However, it is

noteworthy that as the scan lines increase to 8, the detection rate is nearing 90-95% in both the cases of scan band height. It can also be seen that for a band height of 10 pixels, the difference in accuracy between $N_s = 8$ and 4 is less than 20% in each dataset. Therefore, one can decide to go for 4 scan bands instead of 8, trading off accuracy by less than 20% for half the amount of computation cost.

The effectiveness of the proposed technique to detect circular reflectors is illustrated in Fig. 8. It can be seen that a detection accuracy of 85% is obtained using 8 scan bands with each band of 10 pixels high. A comparison on the effect of reducing the number of scan bands and their height is also shown in Fig. 8. It can be seen that reducing the scan band height also reduces the detection rate. For the same number of scan bands but scan band height reduced to 5 pixels, the detection rate has been reduced to about 40%. This is because thinner scan bands fail to completely and conclusively capture the circular reflectors. Therefore, having thicker scan bands and more number of scan bands to sample as many reflectors as possible is desirable to get higher accuracy in the case of circular reflectors.

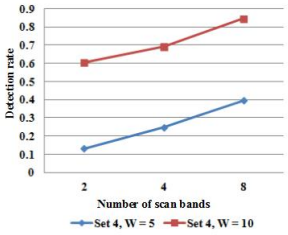

Fig. 8. Detection rate versus number of scan bands for Set 4 with circular reflectors.

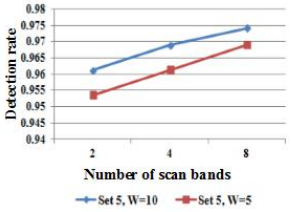

Fig. 9. Detection rate for urban lane scenario with solid lane in Set 5.

Fig. 9 shows the detection rates for varying scan bands to detect solid right lane in urban road context (Set 5). It can be seen that detection rates of over 90% are achieved for all band heights and any number of scan bands. Also, the dataset was chosen such that there are heavy shadows of trees in the images (which usually is the case in most urban road scenarios). These detection rates imply that it is an overkill if more than 4 scan bands are used for detecting solid lanes. This gives us an interesting possibility of merging the information from GPS and road maps, and operate with the required number of scan bands only, if it is known where the vehicle is being driven.

In addition to accuracy, LASeR also allows for low computational complexity as compared to other lane estimation methods. However, this analysis is out of scope of this paper. More analysis on computational complexity of LASeR can be found in [15].

V. Conclusions

In this paper, we proposed LASeR that estimates and tracks lanes by extracting salient lane features from selective scan bands. It is shown that processing narrow bands of the image gives sufficient information because of the saliency of the lane features. A detailed evaluation with ground truth information showed that LASeR gives an error of less than 8 centimeters for ego-vehicle localization on a dataset. The evaluation also showed that having 8 scan bands gives detection rates as high as 95%. As part of future work, it is envisaged to use LASeR for context-aware lane analysis.

Acknowledgment

We acknowledge support of the UC Discovery Program and associated industry partners, especially sponsorship of Korean Electronics Technology Institute and NextChip. We also thank our UCSD LISA colleagues who helped in a variety of important ways in our research studies.

References

[1] M. M. Trivedi, T. Gandhi, and J. McCall, "Looking-In and Looking-Out of a Vehicle: Computer-Vision-Based Enhanced Vehicle Safety," *IEEE Transactions on Intelligent Transportation Systems*, vol. 8, no. 1, pp. 108–120, Mar. 2007.

[2] J. McCall and M. Trivedi, "Video-Based Lane Estimation and Tracking for Driver Assistance: Survey, System, and Evaluation," *IEEE Transactions on Intelligent Transportation Systems*, vol. 7, no. 1, pp. 20–37, Mar. 2006.

[3] A. Borkar, M. Hayes, and M. T. Smith, "A Novel Lane Detection System With Efficient Ground Truth Generation," *IEEE Transactions on Intelligent Transportation Systems*, vol. 13, no. 1, pp. 365–374, Mar. 2012.

[4] N. Hautière, J. Tarel, and D. Aubert, "Towards fog-free in-vehicle vision systems through contrast restoration," *2007 IEEE Conference on Computer Vision and Pattern Recognition*, pp. 1–8, 2007.

[5] H.-Y. Cheng, B.-S. Jeng, P.-T. Tseng, and K.-C. Fan, "Lane Detection With Moving Vehicles in the Traffic Scenes," *IEEE Transactions on Intelligent Transportation Systems*, vol. 7, no. 4, pp. 571–582, Dec. 2006.

[6] R. Gopalan, T. Hong, M. Shneier, and R. Chellappa, "A Learning Approach Towards Detection and Tracking of Lane Markings," *Intelligent Transportation Systems, IEEE Transactions on*, vol. 13, no. 3, pp. 1088–1098, 2012.

[7] Z. Kim, "Robust Lane Detection and Tracking in Challenging Scenarios," *IEEE Transactions on Intelligent Transportation Systems*, vol. 9, no. 1, pp. 16–26, Mar. 2008.

[8] A. Bar Hillel, R. Lerner, D. Levi, and G. Raz, "Recent progress in road and lane detection: a survey," *Machine Vision and Applications*, Feb. 2012.

[9] S. Sivaraman, S. Member, and M. M. Trivedi, "Integrated Lane and Vehicle Detection , Localization , and Tracking : A Synergistic Approach," *IEEE Transactions on Intelligent Transportation Systems*, pp. 1–12, 2013.

[10] B. W. Tatler, M. M. Hayhoe, M. F. Land, and D. H. Ballard, "Eye guidance in natural vision : Reinterpreting salience," *Journal of Vision*, vol. 11, no. 5, pp. 1–23, 2011.

[11] A. Doshi and M. M. Trivedi, "Head and eye gaze dynamics during visual attention shifts in complex environments." *Journal of vision*, vol. 12, no. 2, pp. 1–15, Jan. 2012.

[12] M. Bertozzi and A. Broggi, "GOLD: a parallel real-time stereo vision system for generic obstacle and lane detection." *IEEE transactions on image processing*, vol. 7, no. 1, pp. 62–81, Jan. 1998.

[13] F. William and E. H. Adelson, "The Design and Use of Steerable Filters," *IEEE Transactions on Pattern Analysis and Machine Intelligence*, vol. 13, no. 9, pp. 891–906, 1991.

[14] R. K. Satzoda, S. Martin, M. V. Ly, P. Gunaratne, and M. M. Trivedi, "Towards Automated Drive Analysis : A Multimodal Synergistic Approach," in *IEEE Intelligent Transportation Systems Conference*, 2013, p. To appear.

[15] R. K. Satzoda and M. M. Trivedi, "Vision-based Lane Analysis : Exploration of Issues and Approaches for Embedded Realization," in *2013 IEEE Conference on Computer Vision and Pattern Recognition Workshops on Embedded Vision*, 2013, pp. 598–609.